Tracking Distributions with an Overlap Prior

Ismail Ben Ayed, Shuo Li
GE Healthcare
London, ON, Canada
{ismail.benayed, shuo.li}@ge.com

Ian Ross
London Health Sciences Centre
London, ON, Canada
ian.ross@lhsc.on.ca

Abstract

Recent studies have shown that embedding similarity/dissimilarity measures between distributions in the variational level set framework can lead to effective object segmentation/tracking algorithms. In this connection, existing methods assume implicitly that the overlap between the distributions of image data within the object and its background has to be minimal. Unfortunately, such assumption may not be valid in many important applications.

This study investigates an overlap prior, which embeds knowledge about the overlap between the distributions of the object and the background in level set tracking. It consists of evolving a curve to delineate the target object in the current frame. The level set curve evolution equation is sought following the maximization of a functional containing three terms: (1) an original overlap prior which measures the conformity of overlap between the nonparametric (kernel-based) distributions within the object and the background to a learned description, (2) a term which measures the similarity between a model distribution of the object and the sample distribution inside the curve, and (3) a regularization term for smooth segmentation boundaries. The Bhattacharyya coefficient is used as an overlap measure. Apart from leading to a method which is more versatile than current ones, the overlap prior speeds up significantly the curve evolution. Comparisons and results demonstrate the advantages of the proposed prior over related methods, and its usefulness in important applications such as the left ventricle tracking in Magnetic Resonance (MR) images.

1. Introduction

Object segmentation and tracking in image and image sequences occurs as a fundamental early vision processing task in many important applications. The variational level set framework has led to effective segmentation/tracking algorithms [1]-[18]. It has become very popular in computer vision for several reasons: (a) the solution is sought following the optimization of a global cost functional which balances the influence of image data and prior knowledge in a flexible, principled, and transparent way; (b) the level set representation handles implicitly arbitrary variations in object topology, shape, scale and localization; (c) the obtained results are promising. Level set segmentation and tracking consist of evolving a curve to delineate the target object in the current image. It divides the image domain in two regions: region inside the curve (foreground), which corresponds to the target object at convergence, and region outside the curve (background). The curve evolution equation is obtained by optimizing a functional which, generally, contains a data term measuring the conformity of the observed photometric data within each region to a given statistical description. In most of existing region-based level set methods, the data term can be posed following the Maximum Likelihood (ML) principle [1]-[9]. This corresponds to maximizing the conditional probability of the data given the assumed model distributions within the object and its background. The way of estimating the model distributions divides level set methods into two categories: purely data driven methods, i.e, the model distributions are estimated from the current image along with the segmentation process [6]-[9], [13]-[15], and methods using photometric priors[1] [2]-[5], [10]-[12], i.e., the model distributions are learned *a priori* from a set of segmented training images. Embedding photometric priors in likelihood-based curve evolution has significantly improved the performances of purely data driven methods [1]. It has led to promising results in texture segmentation [4], medical image segmentation [5], and tracking [3]. Unfortunately, likelihood-based curve evolution is sensitive to inaccuracies in estimating the model distributions [13]. Furthermore, it can not incorporate information about the *overlap* between the distributions of photometric variables within the object and the background. Embedding such information in level set segmentation/tracking is the main focus of the current study.

[1] Segmenting images with similar photometric patterns occurs in important applications such as medical image analysis [2], [5]. In this case, learning model distributions from segmented training images is very useful. For object tracking, model distributions can be learned from previously segmented frames [10]-[12].

978-1-4244-2243-2/08/$25.00 ©2008 IEEE

Recent studies have shown the advantages and effectiveness of using *similarity/dissimilarity* measures between distributions in level set segmentation [13]-[15] and tracking [10]-[12]. Possible measures include the Bhattacharyya coefficient [12], [13] and the mutual information [10], [15]. However, the Bhattacharyya coefficient has shown superior performances over other criteria [12], [13]. In [13], level set segmentation is stated as minimizing the *similarity* (or maximizing the *dissimilarity*) between the distributions sampled from inside and outside the curve. In [10], [11], the target object is identified as the region whose sample distribution most closely matches a model distribution. This corresponds to maximizing a functional which measures the similarity between the sample distribution inside the curve and a model distribution of the object. Similar to likelihood-based methods using photometric priors, the model distribution of the object is learned beforehand from training images. The performance of these methods based on *foreground matching* was improved in [12] by adding a *background mismatching* term to the maximized functional. The latter aims to maximize the dissimilarity between the sample distribution of the background and the model distribution of the object. It has been demonstrated experimentally [12] that curve evolution based on the Bhattacharyya measure outperforms the ML principle when dealing with cluttered backgrounds. Furthermore, it is much less sensitive to inaccuracies in estimating model distributions [13].

The current study is related to the level set segmentation/tracking investigations using similarity/dissimilarity measures between distributions [10]-[15]. It is most related to the tracking methods based on photometric priors [10]-[12]. In this connexion, existing methods (for example [10]-[15]) are based on the following implicit assumption: *The overlap between the distributions of image data within the object and its background in the current image/frame has to be minimal.* Unfortunately, such assumption may not be valid in many important applications. Although those methods have been effective in some cases, they are not *versatile* enough to deal with situations in which a "significant" (cf. the left ventricle example in Fig. 1) overlap exists between the distributions within the object and the background. As we will show in the experiments (section 3), embedding prior knowledge of such overlap in the tracking functional would be very useful in important applications. It leads to a method which is more widely applicable than existing ones. In this study, we investigate such a prior.

We develop a variational level set tracking method which embeds knowledge about the overlap between the distributions of the target object and the background. Our solution is sought following the maximization of a functional containing three terms: (1) an original *overlap prior* which measures the conformity of overlap between the nonparametric (kernel-based) distributions within the object and the background according to a learned description, (2) a model matching term which measures the similarity between a model distribution of the object and the sample distribution inside the curve, and (3) a regularization term for smooth segmentation boundaries. The Bhattacharyya coefficient is used as an overlap measure[2]. The functional maximization is obtained by the Euler-Lagrange equations of curve evolution, and efficiently implemented vis level sets. The remainder of this paper is organized as follows. The next section presents the functional, the equation of its maximization, and a simple interpretation of the *overlap prior influence*. Section 3 describes comparisons and results. It shows practical cases in which the proposed functional is advantageous over existing ones. Section 4 contains a conclusion.

2. Formulation

Let $I : \Omega \subset \mathbb{R}^2 \rightarrow \mathcal{Z}$ be an image function from the domain Ω to the space $\mathcal{Z}$ of a photometric variable such as intensity or a color vector. Level set segmentation/tracking consists of evolving a closed planar parametric curve $\vec{\gamma}(s) : [0,1] \rightarrow \Omega$ to delineate a target object in the current image/frame I. It divides Ω into two regions: $\mathbf{R}_{in} = \mathbf{R}_{\vec{\gamma}}$, corresponding to the interior of $\vec{\gamma}$ (foreground), and $\mathbf{R}_{out} = \mathbf{R}_{in}^c = \mathbf{R}_{\vec{\gamma}}^c$, corresponding to the exterior of $\vec{\gamma}$ (background). The curve evolution equation of $\vec{\gamma}$ is commonly obtained by optimizing a cost functional with respect to $\vec{\gamma}$. In this study, we propose to maximize a functional containing three terms.

(1) An overlap prior term

Let P_{in} and P_{out} be the nonparametric[3] (kernel-based) estimates of the distributions of data in the current frame, respectively, inside and outside $\vec{\gamma}$

$$\begin{aligned} \forall z \in \mathcal{Z},\ P_{in}(z) &= \frac{\int_{\mathbf{R}_{in}} K(z - I(x))dx}{a_{in}} \\ P_{out}(z) &= \frac{\int_{\mathbf{R}_{out}} K(z - I(x))dx}{a_{out}} \end{aligned} \quad (1)$$

where a_{in} is the area of region $\mathbf{R}_{in}$: $a_{in} = \int_{\mathbf{R}_{in}} d\mathbf{x}$, and a_{out} is the area of region $\mathbf{R}_{out}$: $a_{out} = \int_{\mathbf{R}_{out}} d\mathbf{x}$. Typical choices of K are the Dirac function and the Gaussian kernel [14]. As in related studies [10]-[12], we assume that the target object is characterized by a model distribution, $\mathcal{M}_{in}$, which can be learned from a relevant, previously segmented frame. Let $B(f, g)$ be the Bhattacharyya coefficient measuring the amount of *overlap* between two statistical sam-

[2] Several studies have found the Bhattacharyya coefficient to be a good measure for segmentation [13], and tracking [19]. Apart from leading to outstanding results, it has a simple analytical expression.

[3] In order to incorporate complex statistical information in the segmentation/tracking functional, the recent trend has been toward using nonparametric models [5], [9]-[16].

ples f and g [13]. Consider

$$B_{out} = B(P_{out}, \mathcal{M}_{in}) = \sum_{z \in \mathcal{Z}} \sqrt{P_{out}(z)\mathcal{M}_{in}(z)} \quad (2)$$

Note that the values of B are always in $[0, 1]$, where 0 indicates that there is no overlap, and 1 indicates a perfect match. B_{out} measures the amount of overlap between the distribution outside the curve (background) and the model distribution of the target object. We assume that a prior estimation of B_{out}, μ_B, is learned beforehand from a previously segmented frame. In order to incorporate information about the photometric similarities between the object and the background, we propose to maximize the following *overlap prior* term which measures the conformity of B_{out} to a learned overlap measure μ_B

$$\mathcal{O} = -\sqrt{(B_{out} - \mu_B)^2} \quad (3)$$

This form of the overlap prior can be viewed as a *generalization* of the *background mismatching* term proposed in [12]. The particular case[4] corresponding to $\mu_B = 0$ reduces (3) to the functional in [12]. The overlap prior is more *versatile* than existing terms. It addresses cases in which an overlap exists between the distributions within the object and the background. As we will show in the experiments, it leads to a method which is more widely applicable than existing ones. In the next section, we will give a simple interpretation of how the overlap prior influences curve evolution.

(2) A model matching term

In conjunction with the overlap prior, we use a foreground matching term which measures the similarity between the distribution inside the curve (foreground) and the model distribution of the target object [11]

$$B_{in} = B(P_{in}, \mathcal{M}_{in}) = \sum_{z \in \mathcal{Z}} \sqrt{P_{in}(z)\mathcal{M}_{in}(z)} \quad (4)$$

(3) A regularization Term

We use a classic regularization term for smooth segmentation boundaries

$$\mathcal{R} = -\oint_{\vec{\gamma}} ds \quad (5)$$

The functional to maximize is a weighted sum of the three terms

$$\begin{aligned} \mathcal{F} &= \alpha\mathcal{O} + \beta B_{in} + \lambda\mathcal{R} \\ &= \underbrace{-\alpha\sqrt{(B_{out} - \mu_B)^2}}_{Overlap\ prior} + \underbrace{\beta B_{in}}_{Model\ matching} \\ &- \underbrace{\lambda \oint_{\vec{\gamma}} ds}_{Smoothness} \end{aligned} \quad (6)$$

[4]The particular case corresponding to $\mu_B = 0$ is an *explicit* form of assuming that the overlap between the distributions of the object and the background is minimal. Such assumption is *implicit* in existing methods.

α, β and λ are positive real constants to balance the contribution of each term.

2.1. Curve evolution equation

The curve evolution equation is obtained following the maximization of $\mathcal{F}$ with respect to $\vec{\gamma}$. To this end, we derive the Euler-Lagrange ascent equation by embedding curve $\vec{\gamma}$ in a one-parameter family of curves: $\vec{\gamma}(s,t) : [0,1] \times \mathbf{R}^+ \rightarrow \Omega$, and solving the partial differential equation:

$$\frac{\partial \vec{\gamma}}{\partial t} = \frac{\partial \mathcal{F}}{\partial \vec{\gamma}} \quad (7)$$

$\frac{\partial \mathcal{F}}{\partial \vec{\gamma}}$ is the functional derivative of $\mathcal{F}$ with respect to $\vec{\gamma}$. After some algebraic manipulations, we have

$$\begin{aligned} \frac{\partial \vec{\gamma}}{\partial t} = \frac{\partial \mathcal{F}}{\partial \vec{\gamma}} &= \underbrace{-\alpha \frac{B_{out} - \mu_B}{\sqrt{(B_{out} - \mu_B)^2}}}_{Overlap\ prior\ influence} \frac{\partial B_{out}}{\partial \vec{\gamma}} \\ &+ \beta \frac{\partial B_{in}}{\partial \vec{\gamma}} + \lambda \frac{\partial \mathcal{R}}{\partial \vec{\gamma}} \end{aligned} \quad (8)$$

Before deriving the final equation, we give a simple interpretation of how the overlap prior guides the curve evolution. The learned overlap measure μ_B influences the sign of the multiplicative coefficient (*overlap prior influence*) affected to the flow $\frac{\partial B_{out}}{\partial \vec{\gamma}}$. This coefficient is *negative* when B_{out} is *superior* to its expected value μ_B. In this case, the overlap prior results in a curve evolution which *decreases* B_{out}. By contrast, when B_{out} is *inferior* to μ_B, the coefficient becomes *positive* and the curve evolution *increases* B_{out}. *The overlap prior leads to a curve evolution which keeps B_{out} close to its expected value.*

To derive the final curve evolution equation, we need to compute $\frac{\partial B_{in}}{\partial \vec{\gamma}}$ and $\frac{\partial B_{out}}{\partial \vec{\gamma}}$. We have

$$\frac{\partial B_{in}}{\partial \vec{\gamma}} = \frac{1}{2} \sum_{z \in \mathcal{Z}} \sqrt{\frac{\mathcal{M}_{in}(z)}{P_{in}(z)}} \frac{\partial P_{in}}{\partial \vec{\gamma}} \quad (9)$$

To compute $\frac{\partial P_{in}}{\partial \vec{\gamma}}$, we use the Euler-Lagrange equations. We can show [8] that, for a scalar function h, the functional derivative with respect to curve $\vec{\gamma}$ of $\int_{\mathbf{R}_{\vec{\gamma}}} h(x)dx$ is $h(x)\vec{n}(x)$, where $\vec{n}$ is the outward unit normal to $\vec{\gamma}$. Applying this result to a_{in} and $\int_{\mathbf{R}_{\vec{\gamma}}} K(z - I(x))dx$ in $\frac{\partial P_{in}}{\partial \vec{\gamma}}$ yields, after some algebraic manipulations

$$\frac{\partial P_{in}(z)}{\partial \vec{\gamma}(s)} = \frac{1}{a_{in}} \left(K(z - I(s)) - P_{in}(s) \right) \vec{n}(s) \quad (10)$$

We assume K is the delta function to simplify the equations. However, the same derivation applies for an arbitrary kernel. Embedding (10) into (9), and after some algebraic manipulations, we obtain:

$$\frac{\partial B_{in}}{\partial \vec{\gamma}(s)} = \frac{1}{2a_{in}} \left(\sqrt{\frac{\mathcal{M}_{in}(s)}{P_{in}(s)}} - B_{in} \right) \vec{n}(s) \quad (11)$$

Similarly, we obtain:

$$\frac{\partial B_{out}}{\partial \vec{\gamma}(s)} = -\frac{1}{2a_{out}} \left(\sqrt{\frac{\mathcal{M}_{in}(s)}{P_{out}(s)}} - B_{out} \right) \vec{n}(s) \qquad (12)$$

Embedding (11), (12), and the derivative of the regularization term [8] in (8) gives the final curve evolution equation:

$$\begin{aligned} \frac{\partial \vec{\gamma}}{\partial t} &= \{ \frac{\alpha}{2a_{out}} \frac{B_{out} - \mu_B}{\sqrt{(B_{out} - \mu_B)^2}} \left(\sqrt{\frac{\mathcal{M}_{in}(s)}{P_{out}(s)}} - B_{out} \right) \\ &+ \frac{\beta}{2a_{in}} \left(\sqrt{\frac{\mathcal{M}_{in}(s)}{P_{in}(s)}} - B_{in} \right) - \lambda\kappa \} \vec{n} \qquad (13) \end{aligned}$$

where κ is the mean curvature function of $\vec{\gamma}$.

2.2. Level-set implementation

We use the level-set formalism [17] to implement the curve evolution equation in (13). Level-set implementation represents curve $\vec{\gamma}$ implicitly by the zero level set of a function $u : \Omega \subset \mathbb{R}^2 \rightarrow \mathbb{R}$ ($\vec{\gamma} = \{u = 0\}$), with the region inside $\vec{\gamma}$ corresponding to $u > 0$. The level-set representation has well-known advantages over an explicit discretization of $\vec{\gamma}$ using a number of points on the curve. It handles automatically topological changes of the evolving curve ($\vec{\gamma}$ may split and merge while u remains a function), and can be effected by stable numerical schemes [17]. One can show that [17] if the curve evolves according to $\frac{\partial \vec{\gamma}}{\partial t} = V.\vec{n}$ (refer to eq. (13)), where $V : \mathbb{R}^2 \rightarrow \mathbb{R}$, then the level set function evolves according to $\frac{\partial u(x,t)}{\partial t} = -V.\|\vec{\nabla} u\|$.

3. Experiments

We conducted a large number of tests to verify the usefulness of the *overlap prior* in important applications. We also performed comparisons to clearly demonstrate the advantages of the proposed functional over related ones. We compared with the functional in [12], and with a likelihood-based functional as in [2], [4]. For comparisons, The same training images, curve initializations, and parameters were used for both methods. Different from existing work, the current experimentation uses examples in which a significant overlap exists between the distributions of the target object and its background (refer for example to Fig. 1 (b)). Parameter μ_b and the model distribution $\mathcal{M}_{in}$ are estimated beforehand in a single training image. As existing methods [5], [11], [12], we employed a leave-one-out technique: the actual images (images of interest) are different from training images. In most of our experiments, we gave the same weight to the overlap and model-matching terms in (6), i.e., $\frac{\alpha}{\beta} = 1$, and we fixed $\lambda = 0.001\alpha$. Note that the set of parameters verifying $\frac{\alpha}{\beta} \in [0.1, 10]$ seems to be an acceptable weighting. Note also that even $\lambda = 0$ would not affect significantly the results. It affects the smoothness of the curve; the higher lambda, the smoother the curve. The photometric variable is color specified in HSV coordinates (examples in Fig. 4), or intensity (examples in Fig. 1, 2, and 3). Color distributions are computed using 4096 bins. Intensity distributions are computed using 255 bins. In the following, we detail comparisons, and give a representative sample of the results.

The first comparison deals with an important application: tracking the left ventricle chamber in MR cardiac sequences. This task is of great interest in automating the diagnosis of cardiovascular diseases [2]. It is still challenging to segment the chamber in the current frame because its intensity profile is similar to the nearby background. The first column in Fig. 1 shows a typical example. Fig. 1 (a) depicts the expected segmentation of the chamber (region inside the red curve) and a region in the nearby background corresponding to the right ventricle (region inside the blue curve). Fig. 1 (b) illustrates the significant overlap between the distributions of these two regions. Generally, general purpose segmentation methods fail in successfully delineating the chamber. The fifth column in Fig. 1 (i and j) depicts the segmentation result *with a likelihood-based functional*. The fourth column (g and h) depicts the segmentation result *with the functional in [12]*. With these two methods, a part of the background, which has an intensity profile similar to the chamber, is included in the final region. This is consistent with the results in [12] showing failure of the method in similar cases. By contrast, *using the overlap prior* delineates accurately the chamber (Fig. 1 (e)), and leads to a region (Fig. 1 (f)) similar to the ground truth (Fig. 1 (d)). The same training image is used for all the methods to learn the model distribution. μ_B corresponds to the Bhattacharyya measure between the object and the background in the training image ($\mu_B = 0.53$). Table 1 reports values of the optimized Bhattacharyya measures at convergence. The proposed method outperforms the method in [12], and those based on the ML principle. Accurate chamber tracking in the rest of the cardiac sequence with the proposed method (using the same model distribution and the same μ_B from a single training image) is shown in Fig. 3. Fig. 3 (a) plots the corresponding optimized Bhattacharyya measures obtained at convergence versus the frame number: Although B_{in} varies, i.e, the true object distribution varies over the sequence, the proposed functional leads to a very accurate tracking due to the positive effect of the overlap prior (B_{out} has approximately a constant value over the sequence). We give here only one typical left ventricle tracking example. The method has been tested with several other examples, and seems to be well-suited to this important application and many other medical applications.

The second comparison and result are depicted in Fig 2 which shows the segmentation of a vehicle in a road sequence frame. The proposed method recovers the target

Method	with the overlap prior ($\mu_B = 0.53$)	without overlap prior ($\mu_B = 0$) [12]	Likelihood
B_{in}	0.98	0.97	0.95
B_{out}	0.54	0.45	0.45

Table 1. Obtained Bhattacharyya measures at convergence for both three methods (left ventricle example in Fig. 1): the proposed functional, i.e., *with the overlap prior*; the functional in [12], i.e., *without the overlap prior*, and a *likelihood-based* functional as in [2], [4].

Method	with overlap prior ($\mu_B = 0.73$)	without overlap prior ($\mu_B = 0$) [12]
B_{in}	0.98	0.98
B_{out}	0.72	0.60
Convergence	1800 iterations	5500 iterations

Table 2. Obtained Bhattacharyya measures at convergence (the vehicle segmentation example): the proposed functional, i.e., *with the overlap prior* ($\mu_B = 0.73$), and the functional in [12], i.e., *without the overlap prior* ($\mu_B = 0$). Bottom row: number of iterations required for convergence.

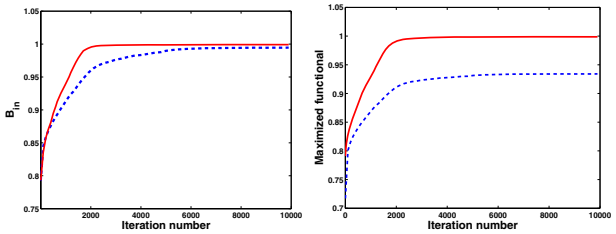

(a) (b)

Figure 5. Maximized measures versus iteration number. Continue: the proposed functional ($\mu_B = 0.73$); discontinue: functional in [12] ($\mu_B = 0$). (a): evolution of the maximized B_{in}; (b): evolution of the overall functional. $\alpha = 0.1\beta$; $\lambda = 0$.

object (the vehicle), whereas the method in [12] incorporates a part of the background inside the final curve (Fig. 2 (d) and (e)). The model distribution and μ_B are estimated from a previous frame ($\mu_B = 0.73$). Curve initialization is shown in Fig. 2 (a), and is arbitrary. This illustrates the robustness of the proposed method with respect to initial conditions. In Fig. 5, we plotted the maximized terms versus the iteration number for both methods, which demonstrates a computational advantage of the overlap prior. *It speeds up significantly the ascent of the maximized terms*. Maximization *with the overlap prior* requires about 1800 iterations to converge, whereas maximization *without the overlap prior* requires about 5500 iterations. Consequently, The proposed functional results in a curve evolution faster than with functional in [12]. Table 2 reports values of the optimized measures at convergence for both methods. This example demonstrates how we can obtain different objects having the same similarity measure with the model distribution. Consequently, matching the distribution inside the curve to a model distribution as in [11] is not sufficient.

In Fig. 4, we show comparisons and results of segmenting an object with an arbitrary shape in the table tennis sequence. Dealing implicitly with arbitrary shapes is an advantage of active curves [11], [12]. Fig. 4 (b) depicts the target object (player arm) in the learning image (frame 6). *With the overlap prior*, the object is recovered in frame 16 (g and h) and frame 26 (i and j). *Without the overlap prior*, i.e., with the method in [12], the racket, which has an intensity profile similar to the arm, is included in the final curve (frame 16: c and d; frame 26: e and f).

4. Conclusion

We investigated an *overlap prior* for object tracking. Comparisons demonstrated that the proposed method outperforms existing ones for situations in which an overlap exists between the distributions of image data within the object and its background. Results showed the usefulness of the overlap prior in important applications. Future investigations include embedding statistical overlap priors in variational object segmentation.

References

[1] D. Cremers, M. Rousson, and R. Deriche. A Review of Statistical Approaches to Level Set Segmentation: Integrating Color, Texture, Motion and Shape. *International Journal of Computer Vision*, 62(3): 249-265, 2007. 1

[2] N. Paragios. A Variational Approach for the Segmentation of the Left Ventricle in Cardiac Image Analysis. *International Journal of Computer Vision*, 50(3): 345-362, 2002. 1, 4, 5

[3] N. Paragios and R. Deriche. Geodesic Active Contours and Level Sets for the Detection and Tracking of Moving Objects. *IEEE Transactions on Pattern Analysis and Machine Intelligence*, 22(3): 266-280, 2000. 1

[4] N. Paragios and R. Deriche. Geodesic Active Regions and Level Set Methods for Supervised Texture Segmentation. *International Journal of Computer Vision*, 46(3): 223-247, 2002. 1, 4, 5

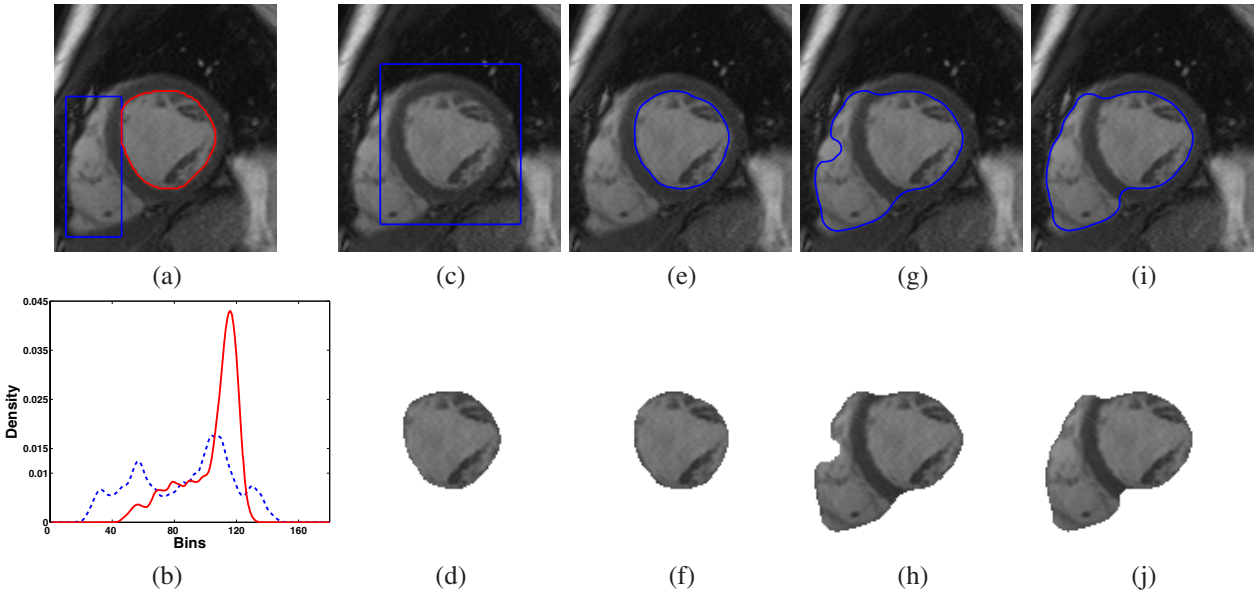

Figure 1. First column: (a) expected segmentation (manually determined by a radiologist) of the left ventricle chamber (red curve); (b) overlap between the distributions of the chamber and the nearby background (region inside the blue curve in (a)). Second column: (c) curve initialization for both methods; (d) ground truth (target object determined by a radiologist). Third column: result obtained with the proposed method, i.e., *with the overlap prior* ((e) final curve (blue), and (f) obtained object). Fourth column ((g) and (h)): result obtained with the method in [12], i.e., *without the overlap prior*. Fifth column: result obtained *with a likelihood-based functional*.

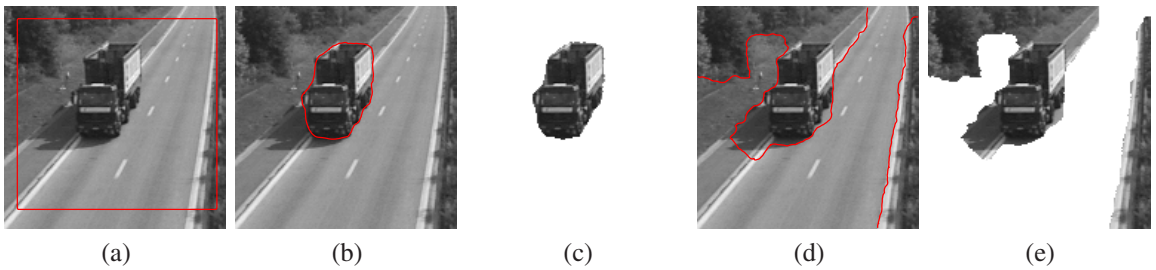

Figure 2. Comparison of a vehicle segmentation in a road sequence. (a): curve initialization for both methods ([12], and the proposed method). (b) and (c): final curve and obtained object *with the proposed method*. (d) and (e): final curve and obtained object *with the method in* [12]. The model distribution and μ_B are estimated from a previous frame. $\mu_B = 0.73$.

[5] M. Rousson, and D. Cremers. Efficient Kernel Density Estimation of Shape and Intensity Priors for Level Set Segmentation. *MICCAI* (2) 2005: 757-764. 1, 2, 4

[6] I. Ben Ayed, N. Hennane, and A. Mitiche. Unsupervised Variational Image Segmentation/Classification using a Weibull Observation Model. *IEEE Transactions on Image Processing*, 15(11): 3431-3439, 2006. 1

[7] T. F. Chan and L. A. Vese. Active Contours without Edges. *IEEE Transactions on Image Processing*, 10(2): 266-277, 2001.

[8] S. C. Zhu and A.L Yuille. Region Competition: Unifying Snake/balloon, Region Growing and Bayes/MDL/Energy for multi-band Image Segmentation. *IEEE Transactions on Pattern Analysis and Machine Intelligence*, 18(9): 884-900, 1996. 3, 4

[9] T. Kadir and M. Brady. Unsupervised Non-parametric Region Segmentation Using Level Sets. *ICCV* 2003: 1267-1274. 1, 2

[10] G. Aubert, M. Barlaud, O. Faugeras, S. Jehan-Besson. Image Segmentation Using Active Contours: Calculus of Variations or Shape Gradients? *SIAM Applied Mathematics*, 63(6): 2128-2154, 2003. 1, 2

[11] D. Freedman and T. Zhang. Active contours for tracking distributions. *IEEE Transactions on Image Processing*, 13(4): 518-526, 2004. 2, 3, 4, 5

[12] T. Zhang and D. Freedman. Improving performance of distribution tracking through background mismatch. *IEEE Transactions on Pattern Analysis and Machine Intelligence*, 27(2): 282-287, 2005. 1, 2, 3, 4, 5, 6, 7

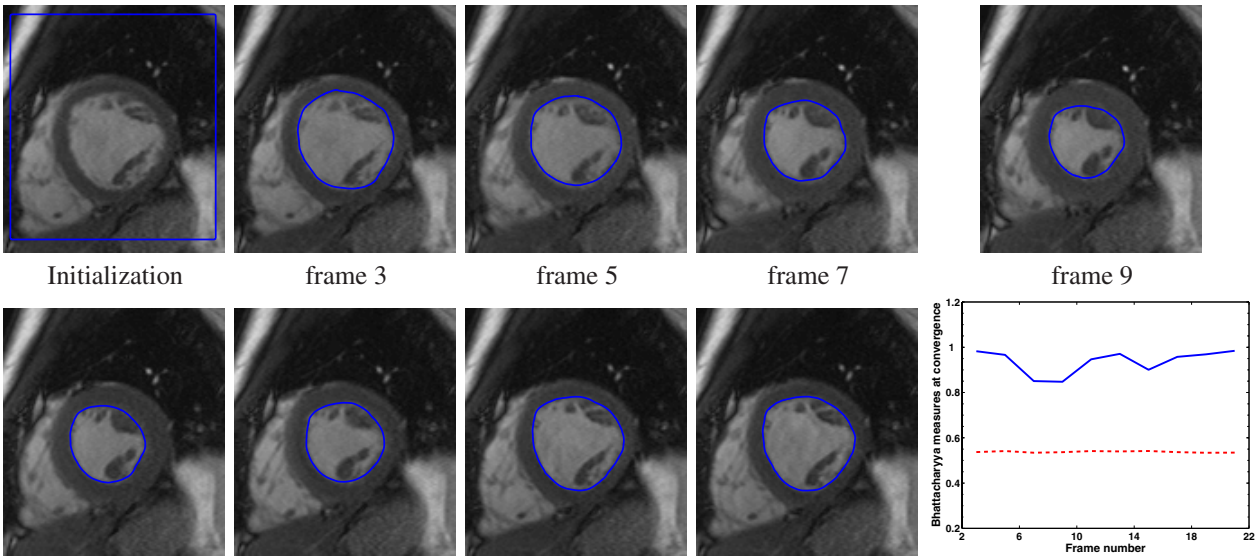

Figure 3. Left ventricle chamber tracking in a cardiac MR sequence. (a) Bhattacharyya measures obtained at convergence versus frame number. B_{in}: continue (blue); B_{out}: discontinue (red). $\alpha = \beta$; $\lambda = 0.001\alpha$.

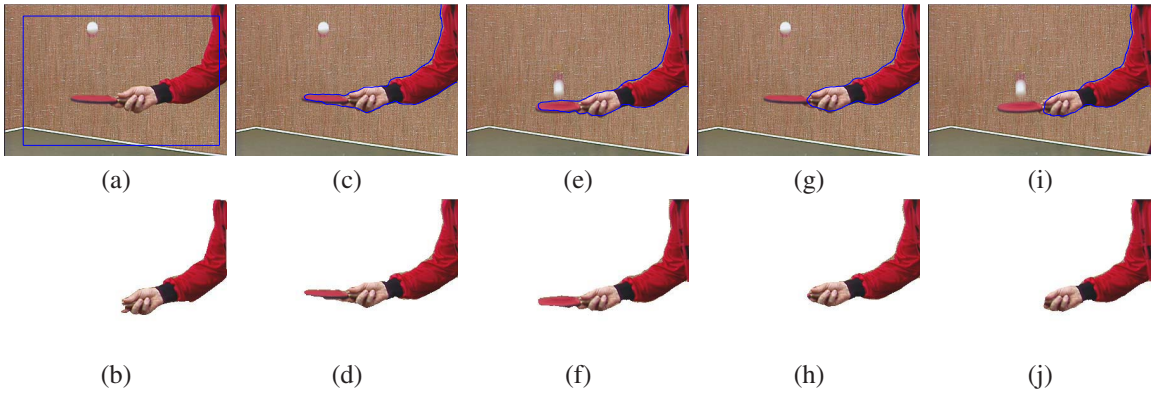

Figure 4. Segmentation of an object with an arbitrary shape in the table tennis sequence (comparisons and results). (a) initialization for both methods (proposed functional and functional in [12]). (b) target object (true object) in the learning image (frame 6). Obtained final curve and segmented object: (c) and (d) in frame 16 *with the method in* [12]; (e) and (f) in frame 26 *with the method in* [12]; (g) and (h) in frame 16 *with the proposed overlap prior*; (i) and (j) in frame 26 *with the proposed overlap prior*.

[13] O. V. Michailovich, Y. Rathi, and A. Tannenbaum. Image Segmentation Using Active Contours Driven by the Bhattacharyya Gradient Flow. *IEEE Transactions on Image Processing*, 16(11): 2787-2801, 2007. 1, 2, 3

[14] T. Georgiou, O. Michailovich, Y. Rathi, J. Malcolm, A. Tannenbaum. Distribution Metrics and Image Segmentation. *Linear Algebra and its Applications*, 425: 663-672, 2007. 2

[15] J. Kim, J. W. Fisher III, A. Yezzi, M. Cetin, and A. S. Willsky. A nonparametric statistical method for image segmentation using information theory and curve evolution. *IEEE Transactions on Image processing*, 14(10): 1486-1502, 2005. 1, 2

[16] S. P. Awate, T. Tasdizen, R. T. Whitaker. Unsupervised Texture Segmentation with Nonparametric Neighborhood Statistics. *ECCV* (2) 2006: 494-507. 2

[17] J.Sethian. Level Set Methods and Fast Marching Methods. *Cambridge University Press*, 1999. 4

[18] D. Cremers. Nonlinear Dynamical Shape Priors for Level Set Segmentation. *CVPR* 2007. 1

[19] D. Comaniciu, V. Ramesh, and P. Meer. Kernel-based object tracking. *IEEE Transactions on Pattern Analysis and Machine Intelligence*, 25(5): 564577, 2003. 2